On Continuation of Inviscid Vortex Patches

Federico Gallizio[1,2], Angelo Iollo[2], Bartosz Protas[3,*], Luca Zannetti[1]

[1] *Dipartimento di Ingegneria Aeronautica e Spaziale*
Politecnico di Torino, 10129 Torino, Italy

[2] *Institut de Mathématiques de Bordeaux UMR 5251 CNRS*
Université Bordeaux 1 and INRIA Futurs MC2, 33405 Talence cedex, France

[3] *Department of Mathematics & Statistics*
McMaster University, Hamilton, Ontario, Canada

Abstract

This investigation concerns solutions of the steady–state Euler equations in two dimensions featuring finite–area regions with constant vorticity embedded in a potential flow. Using elementary methods of the functional analysis we derive precise conditions under which such solutions can be uniquely continued with respect to their parameters, valid also in the presence of the Kutta condition concerning a fixed separation point. Our approach is based on the Implicit Function Theorem and perturbation equations derived using shape–differentiation methods. These theoretical results are illustrated with careful numerical computations carried out using the Steklov–Poincaré method which show the existence of a global manifold of solutions connecting the point vortex and the Prandtl–Batchelor solution, each of which satisfies the Kutta condition.

Key words: Euler equation, vortex patches, existence of solutions, continuation, Steklov–Poincaré iterations
PACS: 47.15.ki, 47.32.Ff

1 Introduction

This work addresses certain fundamental properties of a flow model of interest in the study of massively separated flows past bluff bodies. It is motivated by the field of flow control where one of the recurring themes is the stabilization of unsteady

* Corresponding author. Email: bprotas@mcmaster.ca, Phone: +1 905 525 9140 ext. 24116, Fax: +1 905 522 0935

vortex wakes with applications involving aeronautical or terrestrial vehicles [1]. Stabilization of such flows with a vanishingly small control effort is often based on the premise that there exist steady unstable solutions characterized by recirculation regions with closed streamlines for high enough Reynolds numbers. Therefore, in what follows the flow is considered effectively inviscid, so that the incompressible Euler equation is the relevant model. A further assumption is that the flow is two–dimensional (2D). Despite their simplicity, such models are capable of describing the large–scale vortex dynamics as well as vortex equilibria, and these features are often sufficient to allow for the use of such models as a basis for development of effective control strategies [2]. With such problems in mind, in the present investigation we use a combination of rigorous mathematical analysis and careful numerical computations to address an important theoretical question concerning the Euler equation, namely, the existence of a continuous family of solutions characterized by growing vortex patches.

To fix attention, we consider the flow domain $\Omega \subset \mathbb{R}^2$ as shown in Figure 1 which is motivated by the shape of high–lift devices used in some experimental aeronautical applications (lift is increased as a result of "trapping" a vortex in the cavity [3], see Figure 1). Points belonging to the domain Ω will be denoted $\mathbf{x} = (x,y)$. While in such applications the domain Ω is considered unbounded, in order to avoid technical complications, in the mathematical analysis we will assume without loss of generality that this domain is bounded. The numerical computations reported in this paper use an unbounded domain. The domain boundary is assumed piecewise smooth and not necessarily Lipschitz (i.e., cusps are allowed). Our domain Ω is constructed so that the upstream and downstream boundaries coincide with the OX axis. As a result, this domain may also be used to model flows in the entire plane past *symmetric* obstacles where the OX axis is the axis of symmetry.Expressing the velocity $\mathbf{u}$ in terms of the streamfunction $\psi : \Omega \to \mathbb{R}$ as $\mathbf{u} = [u,v] = \left[\frac{\partial \psi}{\partial y}, -\frac{\partial \psi}{\partial x}\right]$, the two–dimensional (2D) steady–state Euler equation can be rewritten as the following boundary–value problem [4]

$$\boldsymbol{\nabla}^2 \psi = F(\psi) \qquad \text{in } \Omega, \tag{1a}$$

$$\psi = \psi_b \qquad \text{on } \partial\Omega, \tag{1b}$$

where $F : \mathbb{R} \to \mathbb{R}$ is an a priori undefined function, and $\psi_b : \partial\Omega \to \mathbb{R}$ is a function corresponding to the boundary conditions on the normal velocity component. On the parts of the boundary $\partial\Omega$ where the normal velocity vanishes ψ_b is equal to a constant implying that such parts of the boundary are streamlines. On the other hand, on the parts of the boundary where the normal velocity does not vanish (e.g., the inflow and outflow of the channel) ψ_b is obtained by integrating the relationship $\frac{\partial \psi_b}{\partial s} = -\mathbf{u} \cdot \mathbf{n}$, where $\mathbf{n}$ represents the unit normal vector facing out of the domain Ω, and s is the arc–length coordinate parameterizing the domain boundary $\partial\Omega$ and having positive orientation. Equation (1a) expresses the fact that the vorticity $\omega = -F(\psi)$ has a constant value on the streamlines in inviscid 2D time–independent flows. Thus, for regions with closed streamlines, this vorticity is not defined by

the far–field boundary condition (1b) and, as a consequence, system (1) may admit multiple solutions. In principle, each of those vortex solutions could be adopted as a model for a separated flow in the infinite Reynolds number limit, and choosing the relevant one is a long–standing problem in theoretical hydrodynamics; we refer the reader to the monograph [5] for a survey of available results. This multiplicity of solutions is reflected in the different distributions of vorticity $-F(\psi)$ which can be adopted for the region with closed streamlines. Batchelor [6,7] argued that the limiting solution for the viscous flow with the Reynolds number *Re* going to infinity is characterized by $\omega = const$ in the region with closed streamlines, i.e., the finite area wake effectively reduces to a vortex patch. Moreover, in general, solutions with vortex patches may also feature a jump Δh of the Bernoulli constant across the vortex sheet that separates the recirculating flow from the external potential flow. The present study addresses inviscid solutions that in a broad sense belong to the family of such models, also referred to as the Prandtl–Batchelor flows [8]. Inviscid flows described by (1), but construed as limits of certain Navier–Stokes solutions as $Re \to \infty$, can be made unique by taking into account "traces" of viscous phenomena. Indeed, it was shown by Chernyshenko, see e.g. [9], that using the condition that the boundary layer be cyclic removes one degree of freedom in the choice of the problem parameters. For the sake of simplicity, however, we will neglect the vortex sheet at the patch boundary, which is equivalent to setting $\Delta h = 0$. A physical justification for this assumption is that a turbulent mixing layer at a high Reynolds number should cancel the jump of the Bernoulli constant Δh. Thus, the entire steady flow field past a bluff body is then modelled as the coupling of two inviscid flow regions (Figure 1): an irrotational region exterior to the wake, and the wake with $\omega = const$, which in terms of the right–hand side (RHS) in (1a) is expressed as

$$F(\psi) = -\omega H(\alpha - \psi), \tag{2}$$

where $H(\cdot)$ denotes the Heaviside function, ω is the (constant) vorticity, whereas $\alpha \in \mathbb{R}$ is the value the streamfunction ψ assumes on the boundary ∂A of the vortex patch A (cf. Figure 1).

An even simpler model of finite area wakes is provided by point vortices. In this model, the region with closed streamlines is an irrotational flow region with a vortex singularity. As observed by several authors [10–13], vortex patch solutions can be seen as the final result of an accretion process that starts from point vortices. Our point of departure for this work is the following

Conjecture 1 ([14]) *If there is no point vortex in equilibrium that satisfies the Kutta condition, then the associated family of growing patches, including the limiting Prandtl–Batchelor solution, also does not exist.*

We note that this conjecture is in contradiction with some results present in the literature. While it is well know that an inviscid flow past a flat plate broadside to the oncoming stream does not admit any point vortex equilibria (we mention the review paper [15] for some interesting remarks concerning the history of this

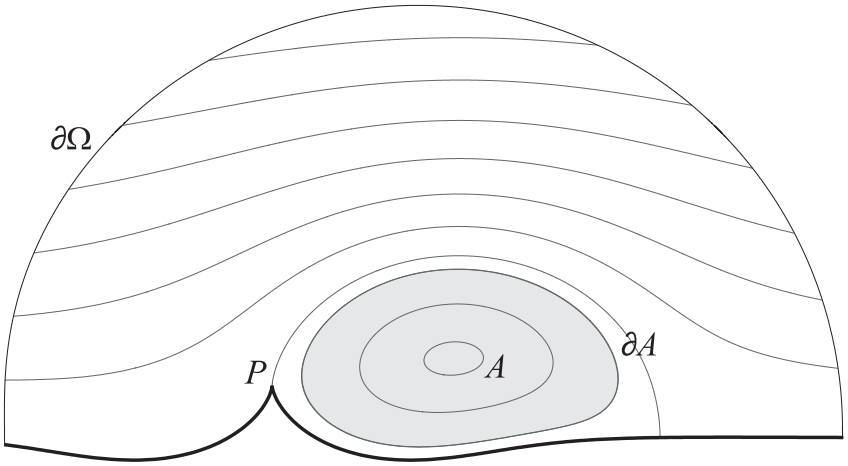

Fig. 1. Schematic of the flow domain: A represents the vortex patch with the boundary ∂A and with a constant vorticity ω embedded in a potential stream, P is the separation point and $\partial\Omega$ the boundary of the flow domain.

problem), Turfus [16] numerically detected finite–area vortex patches in such flow configurations. The existence of a closed wake in the inviscid flow past normal plates was also discussed by Turfus and Castro [17] who demonstrated that a cyclic boundary layer is compatible with the finite area solution determined previously by Turfus. More recently, Castro [18] obtained computational results suggesting possible existence of a second branch in the graph representing the wake size versus the Reynolds number which would extrapolate to a finite area vortex in the limit of an inviscid flow. We also note that results indicating possible existence of solutions contradicting Conjecture 1 were reported in [10]. In an attempt at resolving this conundrum, in the present work we make a step toward proving Conjecture 1 by demonstrating that vortex patch solutions of Euler equation (1)–(2) can in fact be locally continued with respect to parameters. We also remark that related questions concerning existence of continuous families of solutions of system (1)–(2) were addressed, albeit using rather different techniques, in [10]. The structure of this paper is as follows: first in the next section we present a mathematically precise formulation of the problem, in the following section we prove a theorem showing the conditions under continuation of solutions with respect to parameters is possible, in Section 4 this result in generalized for the case of solutions satisfying the Kutta condition; since problem (1)–(2) is nontrivial to solve numerically, a method based on the Steklov–Poincaré iteration is introduced in Section 5, whereas computational results are presented in Section 6; summary and conclusions are deferred to Section 7.

2 Formulation of the Problem

A fundamental property of system (1)–(2) is that the shape of the vortex patch A is not a priori determined and must be found as a part of the solution of the problem. Thus, system (1)–(2) represents a *free–boundary* problem. Since we are going to need this formulation in the sequel, we now rewrite system (1)–(2) in a form that elucidates its free–boundary structure more clearly

$$\nabla^2\psi_1 = -\omega \qquad \text{in } A(\alpha), \tag{3a}$$

$$\nabla^2\psi_2 = 0 \qquad \text{in } \Omega\backslash\overline{A}(\alpha), \tag{3b}$$

$$\psi_1 = \psi_2 = \alpha \qquad \text{on } \partial A(\alpha), \tag{3c}$$

$$\frac{\partial\psi_1}{\partial n} = \frac{\partial\psi_2}{\partial n} \qquad \text{on } \partial A(\alpha), \tag{3d}$$

$$\psi_2 = \psi_b \qquad \text{on } \partial\Omega, \tag{3e}$$

where $\psi_1 = \psi|_A$ and $\psi_2 = \psi|_{\Omega\backslash A}$ are the restrictions of the streamfunction ψ to, respectively, the vortex patch A and its complement in Ω.

Properties of solutions of (1)–(2), or (3), were studied computationally, and in some cases also analytically, by several researchers. It was observed that vortex patch solutions are in fact the result of an accretion process starting from a point vortex solution. The so–called "V–states" arising from desingularization of a single point vortex were studied by Wu, Overman and Zabusky [19], and analytical results concerning the structure of possible singularities of the boundary of the resulting vortex patch were derived in [20]. The case of desingularization of a pair of co–rotating vortices was first investigated by Saffman and Szeto [21]. Two distinct continuous transformations of a co–rotating vortex pair into the Rankine vortex patch were discovered by Cerretelli and Williamson [22], and Crowdy and Marshall [23]. The case of desingularization of a pair of counter–rotating vortices was studied by Pierrehumbert [24] with some details of his computations later rectified by Saffman and Tanveer [25]. A limiting solution in this family which also allows for a vortex sheet on the patch boundary (i.e., in which $\Delta h \neq 0$) is known as the "Sadovskii flow" and was investigated by Sadovskii [26], and then by Moore, Saffman and Tanveer [27]. In regard to desingularization of point vortices in the exterior of an obstacle (a circular cylinder), the paper by the Elcrat et al. [13] is paradigmatic. In that paper the authors considered the Föppl curve pertinent to the flow past a semicircular bump which is the locus of point vortices in a symmetric equilibrium with the obstacle. They showed that each point vortex can be associated with a family of vortex patches with an increasing area $|A| \triangleq \int_\Omega H(\alpha-\psi)\,d\Omega$ (the symbol $\triangleq$ means "equal to by definition") and the same circulation $\Gamma = \omega|A|$ as for the point vortex. Each element of the family can thus be regarded as an inviscid model of a finite–area wake. In such model, the wake is a region with closed streamlines bounded by the body, the symmetry axis and the separatrix streamline separating it from the exterior flow with open streamlines. The vorticity distribution is given

by $\omega = 0$ in the exterior flow and $\omega = \Gamma/|A|$ inside the vortex patch. Assuming $|A|$ to be the parameter defining an element of the family, the point vortex (Föppl) solution will be the first element with $|A| = 0$, and the Prandtl–Batchelor solution will be the last element with $\omega = const$ in the entire region with closed streamlines. In paper [14] the Föppl curve was generalized for the case of flow past a locally deformed wall yielding a locus of point vortices in equilibrium with an arbitrary obstacle. It was also argued in [14] that, as was the case for the semicircular bump, a family of growing vortex patches can be associated with each such point vortex configuration in equilibrium with the obstacle. It was shown as well that when the obstacle has a sharp edge, then the number of such point vortex equilibria which additionally satisfy the Kutta condition is either null or finite. In regard to the first possibility, Conjecture 1 would imply that such obstacles do not admit a finite area wake at high Reynolds numbers. Our present investigation seeks to shed some light on the problem of existence of such families of growing vortex patches from the mathematical point of view. We would like to understand the conditions under which solutions featuring vortex patches can be continued with respect to a parameter. Since parameterization of solutions of (1)–(2) in terms of $|A|$ and/or Γ complicates somewhat the mathematical structure of the problem, for the sake of transparency of our analysis, hereafter we will assume that solutions depend on ω and α which are explicitly present as parameters in the governing system. The first specific question this work intends to answer is thus the following

Question 1 *Given a solution $\psi = \psi(\alpha_0, \omega_0)$ of problem* (1)–(2) *corresponding to the parameter values $\alpha = \alpha_0$ and $\omega = \omega_0$, under what conditions can this solution be continued with respect to one of the parameters ω and α when the other one is held fixed?*

In other words, we want to characterize mathematically the conditions, sufficient or necessary, for the existence of unique neighbor solutions resulting from infinitesimal perturbations of the parameters (Figure 2).

An important in practical applications class of problems (1)–(2) concerns the situation when the solution ψ has a prescribed "separation point", i.e., is subject to the so–called Kutta condition. This condition, commonly used in aeronautical applications, follows from the observation that, for the Reynolds number above a certain value, the viscous flow separates on sharp edges. In the framework of the potential flow theory, the inviscid flow would be singular in the absence of separation, with the flow velocities becoming unbounded at sharp edges. By imposing a prescribed separation point, the Kutta condition simultaneously requires the flow to be regular. Mathematically, this condition is often expressed as follows

$$\lim_{s \to s_0^+} \frac{\partial \psi}{\partial n}(s) = - \lim_{s \to s_0^-} \frac{\partial \psi}{\partial n}(s) < \infty, \tag{4}$$

where s_0 is the arc–length coordinate characterizing the location of the cusp. Relation (4) expresses the fact that, when the Kutta condition is satisfied, the tangential

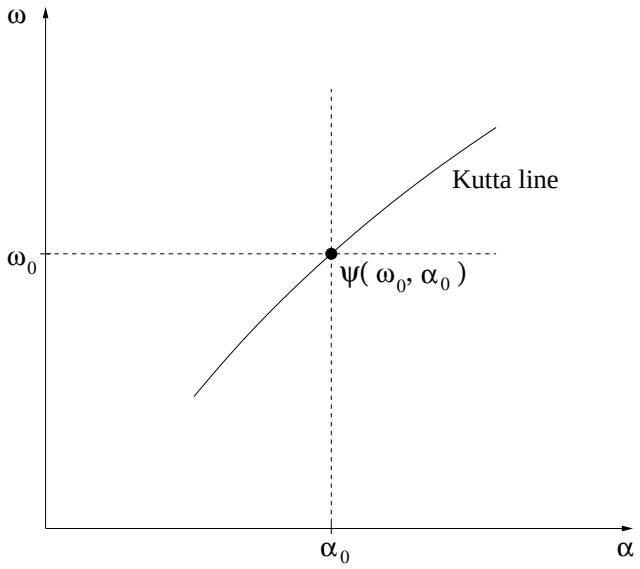

Fig. 2. Schematic of the dependence of the solution ψ of system (1)–(2) on the parameters α and ω: (dashed line) when one of the parameters is held fixed, and (solid line) when Kutta condition (5) is imposed.

velocities on both sides of the cusp are in the limit the same and bounded. Since condition (4) is rather awkward to handle in our analysis, we will use another, approximate, formulation. Since the tangential velocity at the cusp is thus well–defined, we can extrapolate the value of the streamfunction from the cusp $P \in \partial\Omega$ into the flow domain, i.e.,

$$\psi\big|_{P+\varepsilon\mathbf{t}} = \psi_b, \tag{5}$$

where $\varepsilon > 0$ is a small number, whereas $\mathbf{t}$ is the unit tangent vector at P, so that $(P+\varepsilon\mathbf{t}) \in \Omega$. We add that in the actual numerical computations, original form (4) of the Kutta condition will be used (see Section 5 for details). Evidently, imposing the Kutta condition constraints the two–parameter family of solutions, so that a one–parameter family could be expected, although the existence of such families in certain important cases is still an open problem [14]. Thus, the second question we would like to answer in this work can be framed as follows:

Question 2 *Given a solution ψ of problem* (1)–(2) *which in addition satisfies also the Kutta condition* (5)*, under what conditions can this solution be continued with respect to α or ω?*

Locus of solutions constrained by (5) is indicated as the "Kutta line" in Figure 2.

We will address these two questions using a combination of some elementary methods of functional analysis and the theory of elliptic partial differential equations (PDEs). More specifically, we will do this in Section 3 in the following steps:

(1) use a suitable weak formulation of system (1)–(2) to construct an implicit function of the parameters α and ω,

(2) employ the Implicit Function Theorem in the Banach space to determine conditions under which continuation is possible; use the "shape–differential" calculus to determine the Jacobian (perturbation equation) required in the statement of this theorem,
(3) use the Lax–Milgram Theorem together with some standard estimates to determine sufficient conditions under which the Jacobian of the implicit function is invertible.

In addition, one more step will be required in order to answer Question 2 in Section 4, namely:

(4) linearize Kutta condition (5) and use the maximum principle to show that this condition can be always satisfied.

3 Continuation with Respect to Parameters

We begin by stating a weak formulation of Euler equation (1)–(2). For problems with inhomogeneous boundary conditions first we need to perform "lifting" to transform the problem to a form with the homogeneous boundary conditions. We do this here by introducing an auxiliary function $\Theta : \Omega \to \mathbb{R}$ defined as a solution of the following problem

$$\nabla^2\Theta = 0 \qquad \text{in } \Omega, \tag{6a}$$
$$\Theta = \psi_b \qquad \text{on } \partial\Omega. \tag{6b}$$

Expressing the streamfunction as $\psi = \phi + \Theta$ in (1)–(2) yields an equivalent boundary value problem for the function $\phi : \Omega \to \mathbb{R}$ with *homogeneous* Dirichlet boundary conditions, namely

$$\nabla^2\phi = -\omega H(\alpha - \phi - \Theta) \qquad \text{in } \Omega, \tag{7a}$$
$$\phi = 0 \qquad \text{on } \partial\Omega. \tag{7b}$$

Assuming now that the function ϕ and the test function φ belong to the Sobolev space $H_0^1(\Omega)$ of functions with square–integrable gradients and bounded support in Ω [28], the corresponding weak formulation of (7) becomes

$$\phi \in H_0^1(\Omega), \qquad \int_\Omega \nabla\phi \cdot \nabla\varphi \, d\Omega - \omega \int_A \varphi \, d\Omega = 0, \qquad \forall\, \varphi \in H_0^1(\Omega). \tag{8}$$

The existence of solutions of problems of this type was considered, for example, in [29]; it is also supported by ample computational evidence which was reviewed in Introduction. We will thus assume that for some parameter values $\alpha = \alpha_0$ and $\omega = \omega_0$ there exists a solution $\phi_0 = \phi(\alpha_0, \omega_0)$ of problem (8), and we are now interested in the conditions under which this solution ϕ_0 can be uniquely continued

with respect to one of the parameters (Figure 2). We also emphasize that the auxiliary function Θ does not depend on the parameters α and ω. To focus attention, we will therefore fix the value of vorticity ω_0, and will consider the solution to be a function α only, i.e., $\phi = \phi(\alpha)$. Weak formulation (8) can then be represented using an implicit function $\mathcal{G} : H_0^1 \times \mathbb{R} \to \mathbb{R}$ as $\mathcal{G}(\phi, \alpha) = 0$. Local existence of such one–parameter family of solutions $\phi(\alpha)$ is addressed by the Banach space version of the Implicit Function Theorem [30]

Theorem 1 (Implicit Function Theorem) *If X, Y, Z are Banach spaces, $U \subseteq X \times Y$ is an open set, $(x_0, y_0) \in U$, $f : U \to Z$ is a continuous differentiable function, $f(x_0, y_0) = 0$ and $D_y f(x_0, y_0) \in \mathcal{L}(Y; X)$ is invertible with a continuous inverse, then there exist neighborhoods U_1 of x_0 and U_2 of y_0, such that $U_1 \times U_2 \subseteq U$ and a unique continuously differentiable function $g : U_1 \to U_2$, such that*

$$f(x, g(x)) = 0, \qquad \forall x \in U_1 \tag{9}$$

and

$$Dg(x) = -[D_y f(x, g(x))]^{-1} D_x f(x, g(x)), \qquad \forall x \in U_1, \tag{10}$$

where $\mathcal{L}(Y, X)$ is the vector space of all bounded linear operators from Y into X, whereas $D_x f$ and $D_y f$ denote the partial Fréchet derivatives with respect to the first and second variable.

Theorem 1 can be applied to our problem by identifying the Banach space X with our solution space $H_0^1(\Omega)$, and the Banach spaces Y, Z with $\mathbb{R}$. The implicit function f will then represent the weak formulation (8), i.e., $\mathcal{G}(\phi, \alpha) = 0$. Clearly, for this theorem to apply, we have to ensure that the Jacobian $D_\phi \mathcal{G}(\phi, \alpha)$ of the implicit function is an invertible operator with a continuous inverse. The first step towards this end is to identify the form of the Jacobian $D_\phi \mathcal{G}(\phi, \alpha)$. As is evident from formulation (3), our system is of the free–boundary type, and therefore its differentiation with respect to a parameter must be carried out with care. One reason is that when the vortex patch boundary ∂A is perturbed, this also affects the location of where the boundary (interface) conditions (3b) and (3c) are imposed. These issues are addressed by the shape–differential calculus which is a suite of mathematical techniques allowing one to differentiate PDEs defined in variable domains. Below we summarize the main facts only which are relevant to our problem, and refer the reader to the monograph [31] for further details. Let $\phi'_\alpha \triangleq \frac{\partial \psi}{\partial \alpha}\big|_{\alpha=\alpha_0}$ denote the perturbation variable obtained by varying the parameter α while keeping the other parameter ω constant (it corresponds to the quantity $Dg(x)$ appearing in the statement of the Implicit Function Theorem). We assume there exists a vector field $\mathbf{Z} : \Omega \to \mathbb{R}^2$ such that $\mathbf{Z} \cdot \mathbf{n}|_{\partial\Omega} \equiv 0$. When the parameter α is perturbed, i.e., $\alpha = \alpha_0 + \alpha'$, the resulting perturbed vortex patch boundary $\partial A(t, \mathbf{Z})$ can be represented as follows

$$\mathbf{x}(t, \mathbf{Z}) = \mathbf{x} + t\mathbf{Z} \qquad \text{for } \mathbf{x} \in \partial A(0), \qquad t \in \mathbb{R}, \tag{11}$$

where $\partial A(0)$ is the boundary of the unperturbed patch. Integrals defined on such variable domains, e.g., the second term in weak formulation (8), are shape–differentiated as follows [31]

$$\left(\int_{A(t,\mathbf{Z})} \sigma\, d\Omega\right)' = \int_{A(0)} \sigma'\, d\Omega + \oint_{\partial A(0)} \sigma(\mathbf{Z}\cdot\mathbf{n})\, ds, \tag{12}$$

where $\sigma : A(t,\mathbf{Z}) \to \mathbb{R}$ denotes the integrand expression and σ' is its shape derivative. Applying this result to differentiate (8) we obtain

$$\begin{aligned} \frac{d}{d\alpha}\mathcal{G}(\phi(\alpha),\alpha) &= [D_\phi \mathcal{G}(\phi,\alpha)]\phi'_\alpha + D_\alpha \mathcal{G}(\phi,\alpha) \\ &= \int_\Omega \boldsymbol{\nabla}\phi'_\alpha \cdot \boldsymbol{\nabla}\varphi\, d\Omega - \omega_0 \oint_{\partial A} \varphi(\mathbf{Z}\cdot\mathbf{n})\, ds, \qquad \forall \varphi \in H_0^1(\Omega). \end{aligned} \tag{13}$$

We now proceed to relate the perturbation field $(\mathbf{Z}\cdot\mathbf{n})$ appearing in the second integral in (13) with the perturbations of the parameter α. We do this by shape–differentiating boundary condition (3c) which defines the position of the vortex patch boundary

$$\frac{d\psi}{d\alpha}\Big|_{\partial A(t,\mathbf{Z})} = \psi'_\alpha\big|_{\partial A(0)} + \frac{\partial\psi}{\partial n}\Big|_{\partial A(0)}(\mathbf{Z}\cdot\mathbf{n}) = \phi'_\alpha\big|_{\partial A(0)} + \frac{\partial\psi}{\partial n}\Big|_{\partial A(0)}(\mathbf{Z}\cdot\mathbf{n}) = \frac{d\alpha}{d\alpha} = 1, \tag{14}$$

where we used the fact that $\Theta'_\alpha \equiv 0$, so that

$$\mathbf{Z}\cdot\mathbf{n} = \frac{1-\phi'_\alpha\big|_{\partial A(0)}}{\frac{\partial\psi}{\partial n}\big|_{\partial A(0)}}, \tag{15}$$

where we also make the assumption, to be formalized later, that $\frac{\partial\psi}{\partial n}\big|_{\partial A(0)} \neq 0$. Using (15) in (13) we can transform the latter expression to

$$\phi'_\alpha \in H_0^1(\Omega), \qquad \underbrace{\int_\Omega \boldsymbol{\nabla}\phi'_\alpha \cdot \boldsymbol{\nabla}\varphi\, d\Omega + \omega_0 \oint_{\partial A} \left(\frac{\partial\psi}{\partial n}\right)^{-1} \phi'_\alpha \varphi\, ds}_{[D_\phi \mathcal{G}(\phi,\alpha)]\phi'_\alpha} = \underbrace{-\,\omega_0 \oint_{\partial A} \left(\frac{\partial\psi}{\partial n}\right)^{-1} \varphi\, ds}_{D_\alpha \mathcal{G}(\phi,\alpha)}, \qquad \forall \varphi \in H_0^1(\Omega), \tag{16}$$

which we symbolically express in the "strong" for as

$$\left[-\boldsymbol{\nabla}^2 + \omega_0 \left(\frac{\partial\psi}{\partial n}\right)^{-1}\Big|_{\partial A(0)} \delta(\mathbf{x}\big|_{\partial A(0)} - \mathbf{x})\right] \phi'_\alpha = \left(\frac{\partial\psi}{\partial n}\right)^{-1}\Big|_{\partial A(0)} \delta(\mathbf{x}\big|_{\partial A(0)} - \mathbf{x}) \qquad \text{in } \Omega, \tag{17a}$$

$$\phi'_\alpha = 0, \qquad \text{on } \partial\Omega. \tag{17b}$$

Equations (16) and (17) represent, respectively, the weak and strong form of the perturbation of Euler equation (7) resulting from variations of the parameter α. Using the same techniques it can be shown that in the case when we vary the vorticity

ω, and the parameter $\alpha = \alpha_0$ is held fixed, the perturbation equation involves the same operator $[D_\phi \mathcal{G}]$, and takes the form

$$\phi'_\omega \in H^1_0(\Omega), \qquad \int_\Omega \boldsymbol{\nabla}\phi'_\omega \cdot \boldsymbol{\nabla}\varphi \, d\Omega + \omega_0 \oint_{\partial A} \left(\frac{\partial \psi}{\partial n}\right)^{-1} \phi'_\omega \varphi \, ds = \int_A \varphi \, ds \qquad \forall \varphi \in H^1_0(\Omega), \tag{18}$$

which we symbolically express in the "strong" for as

$$\left[-\boldsymbol{\nabla}^2 + \omega_0 \left(\frac{\partial \psi}{\partial n}\right)^{-1}\Big|_{\partial A(0)} \delta(\mathbf{x}\big|_{\partial A(0)} - \mathbf{x})\right] \phi'_\omega = H(\alpha_0 - \psi) \qquad \text{in } \Omega, \tag{19a}$$

$$\phi'_\omega = 0, \qquad \text{on } \partial\Omega \tag{19b}$$

where $\phi'_\omega \triangleq \frac{\partial \phi}{\partial \omega}\big|_{\alpha=\alpha_0}$.

Given perturbation equations (16) and (18), the next step is to determine the conditions under which the associated Jacobian operator $[D_\phi \mathcal{G}(\phi, \alpha)]$ is invertible. To this end we will employ the Lax–Milgram Theorem which provides the sufficient conditions for existence of solutions of elliptic boundary value problems of the type (16) and (18). Assuming now that H is a real Hilbert space with $\|\cdot\|$ denoting its norm, $(\cdot,\cdot)$ its inner product, and $\langle\cdot,\cdot\rangle$ the pairing with its dual space, we have the following

Theorem 2 (Lax–Milgram, [32]) *Assume that*

$$\mathcal{B} : H \times H \to \mathbb{R}$$

is a bilinear mapping for which there exist constants $\xi, \eta > 0$ *such that*

$$|\mathcal{B}[w_1, w_2]| \leq \xi \|w_1\| \|w_2\|, \qquad \forall w_1, w_2 \in H, \tag{20a}$$

$$\eta \|w\|^2 \leq \mathcal{B}[w, w], \qquad \forall w \in H. \tag{20b}$$

Finally, let $\mathcal{T} : H \to \mathbb{R}$ *be a bounded linear functional on* H*. Then, there exists a unique element* $w_0 \in H$ *such that*

$$\mathcal{B}[w_0, w] = \langle \mathcal{T}, w \rangle, \qquad \forall w \in H.$$

In our problem the Hilbert space H can be identified with the solution space $H^1_0(\Omega)$, whereas the bilinear form $\mathcal{B}$ with the weak form of the Jacobian (16) [resp. (18)] regarded as a function of both the perturbation variable ϕ'_α (resp. ϕ'_ω) and the test function φ, i.e., $\mathcal{B}[\phi'_\alpha, \varphi] = [D_\phi \mathcal{G}](\phi'_\alpha, \varphi)$ [resp. $\mathcal{B}[\phi'_\omega, \varphi] = [D_\phi \mathcal{G}](\phi'_\omega, \varphi)$]. Thus, in order to establish invertibility of the Jacobian, we need to demonstrate boundedness (20a) and coercivity (20b) of this bilinear form.

To fix attention we will focus on problem (16). As regards boundedness, we first apply the Cauchy–Schwarz inequality to the first term on the left–hand side (LHS)

in (16)

$$\Big|\int_\Omega \boldsymbol{\nabla}\phi'_\alpha\cdot\boldsymbol{\nabla}\varphi\,d\Omega\Big| \le \left[\int_\Omega (\boldsymbol{\nabla}\phi'_\alpha)^2\,d\Omega\right]^{1/2}\left[\int_\Omega (\boldsymbol{\nabla}\varphi)^2\,d\Omega\right]^{1/2} \le \|\phi'_\alpha\|_{H^1_0(\Omega)}\|\varphi\|_{H^1_0(\Omega)}. \tag{21}$$

Next we introduce the following

Assumption 1 *There exist constants $U_{max} \ge U_{min} > 0$ such that*

$$\operatorname{sign}(\omega_0)\frac{\partial\psi}{\partial n} \le U_{max} \qquad \text{a.e. on } \partial A, \tag{22a}$$

$$\operatorname{sign}(\omega_0)\frac{\partial\psi}{\partial n} \ge U_{min} \qquad \text{a.e. on } \partial A. \tag{22b}$$

The constants U_{min} and U_{max} thus represent an upper and lower bound on the tangential velocity component on the vortex patch boundary ∂A. By examining a simple vortex system, e.g., a single point vortex, it is evident that vortices with *positive* circulation induce *positive* azimuthal (tangential) velocity, and vice versa, hence Assumption 1 is justified. Using assumption (22a), the second term on the LHS in (16) can be bounded from above as follows

$$\omega_0 \oint_{\partial A}\left(\frac{\partial\psi}{\partial n}\right)^{-1}\phi'_\alpha\varphi\,ds \le \frac{\omega_0}{U_{min}}\oint_{\partial A}\phi'_\alpha\varphi\,ds. \tag{23}$$

The term on RHS in (23) can be further bounded by applying the Cauchy–Schwarz inequality combined with the obvious estimate $\|f\|_{L_2(\Omega)} \le C\|f\|_{H^1_0(\Omega)}$ with some $C > 0$

$$\oint_{\partial A}\phi'_\alpha\varphi\,ds \le \|\phi'_\alpha\|_{L_2(\partial A)}\|\varphi\|_{L_2(\partial A)} \le C^2\|\phi'_\alpha\|_{H^1_0(\Omega)}\|\varphi\|_{H^1_0(\Omega)}. \tag{24}$$

Combining inequalities (21), (23), and (24) we obtain for the bilinear form

$$\big|[D_\phi\mathcal{G}](\phi'_\alpha,\varphi)\big| \le (1+\frac{\omega_0}{U_{min}}C^2)\|\phi'_\alpha\|_{H^1_0(\Omega)}\|\varphi\|_{H^1_0(\Omega)}, \tag{25}$$

which shows that boundedness condition (20a) is satisfied.

As regards coercivity (V–ellipticity) condition (20b), we proceed as follows

$$\begin{aligned}\forall\phi\in H^1_0(\Omega),\quad [D_\phi\mathcal{G}](\phi,\phi) &= \int_\Omega(\boldsymbol{\nabla}\phi)^2\,d\Omega + \omega_0\oint_{\partial A}\left(\frac{\partial\psi}{\partial n}\right)^{-1}\phi^2\,ds\\ &\ge \int_\Omega(\boldsymbol{\nabla}\phi)^2\,d\Omega + \frac{|\omega_0|}{U_{max}}\oint_{\partial A}\phi^2\,ds\\ &\ge \int_\Omega(\boldsymbol{\nabla}\phi)^2\,d\Omega \ge \xi\|\phi\|_{H^1_0(\Omega)},\end{aligned} \tag{26}$$

where $\xi > 0$ is a constant, and we employed assumption (22b) together with the Poincaré inequality. Estimate (26) shows that, subject to assumption (22b), the co-

ercivity condition (20b) is satisfied, and therefore the Jacobian $[D_\phi \mathcal{G}]$ of the implicit function is invertible. Finally, we need to show that the inverse Jacobian $[D_\phi \mathcal{G}]^{-1}$ is a continuous operator. We do this by combining inequality (20b) with the estimate $\mathcal{B}[w_0, w_0] = \langle f, w_0 \rangle \leq \|f\|_{H^{-1}(\Omega)} \|w_0\|_{H_0^1(\Omega)}$, $w_0 \in H_0^1(\Omega)$, which yields

$$\|w_0\|_{H_0^1(\Omega)} = \|[D_\phi \mathcal{G}]^{-1} f\|_{H_0^1(\Omega)} \leq \frac{1}{\eta} \|f\|_{H^{-1}(\Omega)}. \tag{27}$$

Estimate (27) shows that the inverse Jacobian $[D_\phi \mathcal{G}]^{-1}$ is a continuous, and therefore also bounded [30], operator. Combining Theorems 1 and 2 with inequalities (25) and (26) we thus have a proof of the following

Theorem 3 *Assume conditions* (22) *hold. Then, there is a neighborhood of the point* (α_0, ω_0) *in which there exist smooth families* $\psi = \psi(\alpha, \omega_0)$ *and* $\psi = \psi(\alpha_0, \omega)$ *of solutions to problem* (1)–(2) *depending, respectively, on the parameters* α *and* ω.

4 Continuation in the Presence of Kutta Condition

Our next goal is to consider conditions under which continuation of solutions is possible subject to Kutta condition (5) which restricts the set of solutions to a one–parameter family. Before we can do this, we need to address one technical difficulty, namely, the fact that Kutta condition (5) requires the solution of problem (1)–(2) to be defined at any, in principle arbitrary, point $(P + \varepsilon \mathbf{t}) \in \Omega$, whereas so far we considered weak solutions only which do not necessarily possess this property. Furthermore, in our subsequent development we will need to employ the maximum principle for the Laplace equation which requires the solutions to be at least C^2. With this in mind, we need to establish that weak solutions of the perturbation equations, whose existence and uniqueness was proved in Theorem 3, are in fact smooth in $\Omega \backslash \overline{A}$, i.e., in the part of the flow domain where Kutta condition (5) may be imposed. As regards the original Euler equation, we note that the solution ψ_2 is defined by (3b), (3c), and (3e), i.e., it satisfies the Laplace equation in $\Omega \backslash \overline{A}$ with the Dirichlet boundary conditions. Regularity of such problems was considered for instance in [33], where it was proved (in Section 4.5) that weak solutions of the Laplace equation in general domains possess in fact the required C^2 regularity in the interior of the domain. This result allows us to justify complementing system (1)–(2) with Kutta condition (5). Since solutions of this augmented system represent a one–parameter family, perturbation of the Kutta condition yields to the first order

$$\psi\big|_{P+\varepsilon\mathbf{t}} + \psi'_\omega\big|_{P+\varepsilon\mathbf{t}} \delta\omega + \psi'_\alpha\big|_{P+\varepsilon\mathbf{t}} \delta\alpha + O\left((\delta\alpha)^2 + (\delta\omega)^2\right) = \psi_b, \tag{28}$$

where $\omega = \omega_0 + \delta\omega$ and $\alpha = \alpha_0 + \delta\alpha$. Assuming to fix attention that $\delta\omega = \delta\omega(\delta\alpha)$, using (5) and neglecting quadratic terms, relation (28) is simplified to the form

$$\delta\omega = \left.\frac{\psi'_\alpha}{\psi'_\omega}\right|_{P+\varepsilon\mathbf{t}} \delta\alpha, \tag{29}$$

which implies that, to the leading order, the vorticity perturbations $\delta\omega$ can be adjusted to the perturbations of the independent parameter α, so that the Kutta condition is satisfied, provided that

$$\psi'_\omega\big|_{P+\varepsilon\mathbf{t}} \neq 0. \tag{30}$$

In the same spirit, assuming that the vorticity ω serves as the independent parameter, i.e., $\delta\alpha = \delta\alpha(\delta\omega)$, we obtain the condition

$$\psi'_\alpha\big|_{P+\varepsilon\mathbf{t}} \neq 0. \tag{31}$$

Since in the domain $\Omega\backslash\overline{A} \ni (P+\varepsilon\mathbf{t})$ the perturbation variables $\psi'_\alpha \equiv \phi'_\alpha$ and $\psi'_\omega \equiv \phi'_\omega$ satisfy the Laplace equations with the homogeneous Dirichlet boundary conditions imposed on $\partial\Omega$ [cf. (17b) and (19b)], it follows from the maximum principle for elliptic PDEs [32] that conditions (30) and (31) are satisfied. With this we have thus proved the following theorem

Theorem 4 *Assume the conditions of Theorem 3 are satisfied. Then, there are neighborhoods of the points* α_0 *and* ω_0 *in which there exist one–parameter families* $\psi = \psi(\alpha) = \psi(\alpha, \omega(\alpha))$ *and* $\psi = \psi(\omega) = \psi(\alpha(\omega), \omega)$ *of solutions to problem* (1)–(2) *subject to additional condition* (5) *which depend, respectively, on the parameters* α *and* ω.

5 Numerical Method

Our objective in this Section is to introduce a method for the numerical solution of problem (1)–(2) in a semi–infinite domain bounded by a wall with a protruding obstacle (Figure 1). The idea of the proposed method is to approximate system (1)–(2) on a suitable grid. The streamline $\psi = \alpha$, which separates the rotational region $A(\alpha)$ from the surrounding irrotational domain $\Omega\backslash\overline{A}(\alpha)$, is not explicitly tracked, but is detected as a jump of the vorticity ω represented on the grid. In general, resolving accurately this separatrix would require a refined grid. Furthermore, since the physical domain extends to infinity, the truncated computational domain should be large in comparison to the size of the vortex patch $A(\alpha)$, and a straightforward application of any standard solution method to the problem in the entire domain would require a very large number of grid points. In addition, some artificial far–field boundary conditions would have to be adopted at the outer boundary to model the inflow/outflow from the truncated domain. On the other hand, when $\psi > \alpha$, equation (1a)–(2) reduces to the Laplace equation which, in general, should not require such a significant computational effort.

The method proposed here overcomes these difficulties by combining a conformal mapping of the physical domain into a suitable transformed plane and the decomposition of the transformed domain into two subdomains, namely:

- a small *interior* subdomain Ω_i which includes the image of the recirculating flow, and
- an *exterior* subdomain Ω_e comprising the remainder of the flow field which extends to infinity.

Briefly, system (1)–(2) is solved numerically by combining a finite–difference approach in the interior subdomain Ω_i with an analytical expression for the solution of the Laplace equation in the exterior subdomain Ω_e. The two solutions are coupled through the boundary conditions on the interface γ_{AB} separating the two subdomains: for the interior subproblem we use the Dirichlet boundary condition $\psi_i = \psi_e$, whereas for the exterior subproblem the Neumann boundary condition $\partial\psi_e/\partial n = \partial\psi_i/\partial n$, where the subscripts i and e refer to the solutions defined on the interior and the exterior subdomains, i.e., $\psi_i \triangleq \psi|_{\Omega_i}$ and $\psi_e \triangleq \psi|_{\Omega_e}$. Repeated solution of such two coupled problems in known as the Steklov–Poincaré iteration which is a well–known approach in the domain decomposition literature [34]. As regards computational efficiency, the fact that one has to perform iterations is offset by a modest number of grid points required to solve the interior subproblem. In the following subsections we describe the two key enablers of the proposed method, namely, the conformal mapping and the solution technique in the transformed domain.

5.1 Conformal Mapping

To fix attention, we consider flows past a wall extending to infinity in the upstream and downstream direction, and featuring a cusped obstacle. An example of such a flow domain is shown in Figure 3a with the interior subdomain Ω_i bounded by a segment of the solid wall and an interface γ_{AB} connecting points A and B. We will show here how, by combining two conformal mappings, such a domain can be transformed to a domain with a simple geometry in which our problem can be solved using standard techniques. According to the Riemann mapping theorem [35], any arbitrary simply–connected region, such as the one shown in Figure 3a, can be conformally mapped onto the upper half plane of a transformed domain. Let us denote z–plane the complex physical plane, where $z = x + iy$ and $i = \sqrt{-1}$, and λ–plane the transformed plane. There exists, thus, a mapping function $z = z(\lambda)$ which maps the real axis of the λ–plane onto an arbitrarily shaped line in the z–plane extending in both directions to infinity, such that the upper half plane in the λ–plane (Figure 3b) is mapped onto the region above the wall in the z-plane.

The flow domain shown in Figure 3a is obtained from the half–plane shown in Fig-

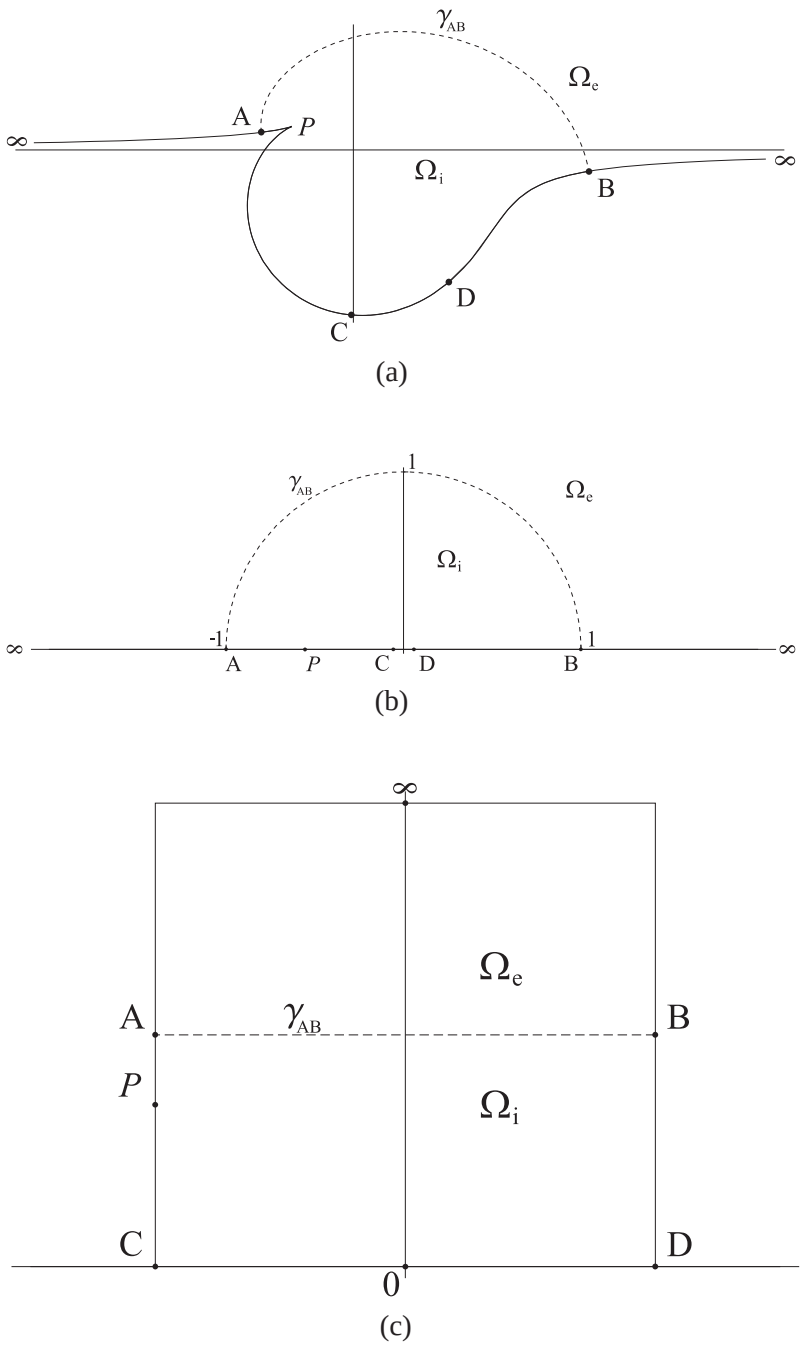

Fig. 3. Domains used in the numerical solution of system (1)–(2): (a) z–plane (the physical domain), (b) λ–plane (the computational domain for the exterior problem), and (c) ζ–plane (the computational domain for the interior problem); in the figures the solid lines represent (the images of) the domain boundaries, whereas the dotted lines represent the interface γ_{AB} separating Ω_i and Ω_e in the three planes.

ure 3b using a simple variation of *Ringleb's snow–cornice mapping* [36], namely

$$z = \frac{\lambda}{a} - b + \frac{\lambda_1^2}{\frac{\lambda}{a} - b - \lambda_1}, \tag{32}$$

where the complex parameter λ_1 defines the shape of the cornice and the two real parameters a and b are such that $z_A = z(-1)$, $z_B = z(1)$ (z_A and z_B are the positions of the points A and B in the z–plane, see Figure 3a). As shown in Figure 3b, in the λ–plane the interior subdomain is mapped into the region inside the unit semi–circle, while the exterior sub–domain is its complement in the upper half–plane.

The second conformal mapping transforms the interior of the rectangle in the ζ–plane (Figure 3c) into the upper half of the λ–plane (Figure 3b) and is based on the Jacobi elliptic sine–amplitude function Sn. In the ζ–plane the interior subdomain corresponds to the lower half of the rectangle and the exterior subdomain corresponds to the upper half of the rectangle (Figure 3c). The mapping function is

$$\lambda = \frac{\mathrm{Sn}(\zeta, m)}{d}, \tag{33}$$

where the real parameters m and d are the elliptic modulus and the scaling factor, respectively. The elliptic modulus m defines the aspect ratio of the rectangle in the ζ–plane through the equation

$$\frac{|\zeta_D - \zeta_C|}{2|\zeta_A - \zeta_C|} = \frac{K(m)}{K'(m)},$$

where $K(m)$ is the complete elliptic integral of the first kind and $K'(m) = K(1-m)$, whereas ζ_A, ζ_C and ζ_D are the coordinates of the points A, C and D in the ζ–plane (Figure 3c). The scaling factor d is a free parameter and its choice determines the coordinates z_C and z_D of the points C and D in the physical plane and the location in the ζ–plane of the image ζ_P of the cusp P.

As described below, system (1)–(2) is solved numerically on an equispaced Cartesian grid defined inside the lower rectangle in the ζ–plane. For an accurate enforcement of the Kutta condition (4), it is convenient to select a value of the parameter m such that the point ζ_P coincides with a grid node. Discretizing the side CA of the rectangle with p grid points and collocating the image of the point P with the n–th node gives

$$\zeta_P = d[-K(m) + \mathrm{i}(n/p)K'(m)],$$

so that (33) becomes

$$\lambda_P = \frac{\mathrm{Sn}[-K(m) + \mathrm{i}\,(n/p)\,K'(m)/2, m]}{\mathrm{Sn}[-K(m) + \mathrm{i}K'(m)/2, m]}$$

which makes it possible to obtain a suitable value of the elliptic modulus m via a trial–and–error approach. An example of the computational grid generated with the procedure described above, albeit coarser than the ones used in the actual computations, is shown in Figure 4. The figure also features a magnification of the region showing the point P coinciding with a grid point.

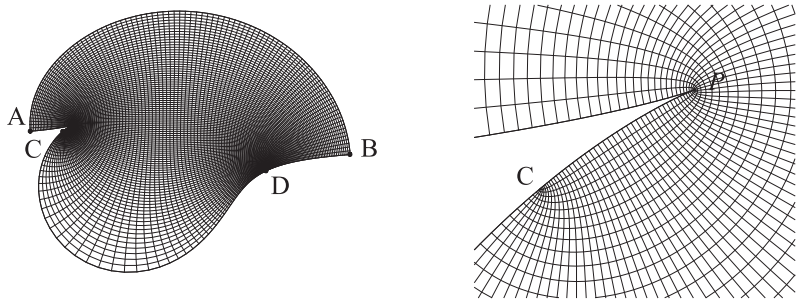

(a) (b)

Fig. 4. Examples of a coarse grid generated by the conformal mapping on the z–plane: (a) in the interior subdomain Ω_i, and (b) magnification of the neighborhood of the cusp P.

5.2 Solution in the Transformed Domain

System (1)–(2) is transformed to the ζ–plane with $\zeta = \xi + i\eta$ acting as the independent variable. Defining $\nabla^2_\zeta \triangleq \partial^2_\xi + \partial^2_\eta$, equation (1a)–(2) becomes

$$\nabla^2_\zeta \psi = \frac{1}{J}[-\omega H(\alpha - \psi)], \tag{34}$$

where $J \triangleq |dz/d\zeta|^2$. The interior subdomain Ω_i coincides with the rectangle *ABCD* whose upper, lower, left and right boundaries are denoted, respectively, γ_{AB}, γ_{CD}, γ_{AC}, γ_{BD}. We will denote Ω_v the rotational portion of the interior subdomain ($\Omega_v \subset \Omega_i$). In the interior subdomain the problem is defined by the following boundary conditions

$$\psi_i = 0 \qquad \text{on } \gamma_{AC} \cup \gamma_{CD} \cup \gamma_{DB}, \tag{35a}$$
$$\psi_i = \psi_e \qquad \text{on } \gamma_{AB}, \tag{35b}$$

where ψ_e is the Dirichlet boundary condition expressed in terms of the solution in the exterior subdomain Ω_e. The proposed method is based on the Schauder fixed point theorem [30]. Let the streamfunction be defined by

$$\psi_i = \psi^0 + \omega\psi^1, \qquad \text{in } \Omega_i, \tag{36}$$

where ψ^0 satisfies the system with a homogeneous RHS and inhomogeneous boundary conditions, i.e.,

$$\nabla^2_\zeta \psi^0 = 0 \qquad \text{in } \Omega_i, \tag{37a}$$
$$\psi^0 = 0 \qquad \text{on } \gamma_{AC} \cup \gamma_{CD} \cup \gamma_{DB}, \tag{37b}$$
$$\psi^0 = \psi_e \qquad \text{on } \gamma_{AB}, \tag{37c}$$

whereas ψ^1 satisfies the system with an inhomogeneous RHS and homogeneous boundary conditions, i.e.,

$$\nabla^2_\zeta \psi^1 = 0 \qquad \text{in } \Omega_i \backslash \Omega_v, \tag{38a}$$

$$\nabla^2_\zeta \psi^1 = \frac{1}{J} \qquad \text{in } \Omega_v, \tag{38b}$$

$$\psi^1 = 0 \qquad \text{on } \gamma_{AC} \cup \gamma_{CD} \cup \gamma_{DB} \cup \gamma_{BA}. \tag{38c}$$

The vorticity ω is computed by imposing the Kutta condition at the cusp ζ_P. We note that condition (4) implies the following relation in the transformed ζ–plane

$$\frac{\partial \psi}{\partial \xi}\Big|_{\zeta_P} = 0. \tag{39}$$

We also observe that discretizing the derivative in (39) with a finite–difference formula yields approximate relation (5). In the interior subdomain, the algorithm consists in iterating the equation

$$\nabla^2_\zeta \psi_{n+1} = \frac{1}{J}\left[-\omega_n H(\alpha - \psi_n)\right], \qquad n = 1, \ldots, \tag{40}$$

where the subscripts represent the iteration numbers. System (37) is not affected by this iterative procedure, thus ψ^0 is computed only once. With ψ^0 fixed and Ω_v given, ψ^1 and ω can be determined at any given n–th iteration. Then, at the $(n+1)$–th iteration, a new shape of the vortex region Ω_v is determined by the level set $\psi_{n+1} = \alpha$ and the process is repeated until convergence is attained.

On the other hand, the potential flow in the exterior subdomain Ω_e is computed in the λ–plane. Let the complex potential w_e be defined as

$$w_e(\lambda) = Q_\infty \lambda + \sum_{j=1}^{\infty} a_j \lambda^{-j} \tag{41}$$

with

$$Q_\infty = \lim_{\lambda \to \infty} \left(\frac{\mathrm{d}w_e}{\mathrm{d}z}\right)\left(\frac{\mathrm{d}z}{\mathrm{d}\lambda}\right) = \frac{q_\infty}{a},$$

where q_∞ is the asymptotic velocity in the physical plane. In the λ–plane, the exterior subdomain Ω_e corresponds to the region exterior to the unit circle in the upper half–plane. The portion of the real axis with $1 \leq |\lambda| < \infty$ is the image of the solid walls upstream and downstream of the cavity. We see that in order to ensure the impermeability of the solid wall, exterior potential (41) must be such that $\psi = \text{const}$ on the real axis, and as a result the coefficients a_j, $j = 1, \ldots$, must be real. Noting that $\lambda = \rho \exp(i\varphi)$, the problem is closed by enforcing the Neumann boundary condition $(\partial \psi_e / \partial \rho) = (\partial \psi_i / \partial \rho)$ on the common boundary γ_{AB}, with $(\partial \psi_i / \partial \rho)$ expressed in terms of the interior solution ψ_i. We observe that the derivatives in the directions normal to the interface γ_{AB} in the λ–plane and ζ–plane are related through the

following identity

$$\frac{\partial \psi_e}{\partial \rho} = \frac{\partial \psi_i}{\partial \eta}\left|\frac{d\lambda}{d\zeta}\right|^{-1}.$$

Let us set $g(\varphi) = (\partial\psi_i/\partial\rho)_{\rho=1}$. We remark that the interior solution along the common boundary γ_{AB} defines the function $g(\varphi)$ in the interval $0 \le \varphi \le \pi$. To ensure impermeability of the solid walls we therefore need $g(0) = g(\pi) = 0$. Thus, $g(\varphi)$ can be continued on the interval $\pi \le \varphi \le 2\pi$, i.e., on the entire unit circle of the λ–plane, by assuming that $g(\pi+\delta) = -g(\pi-\delta)$, with $0 \le \delta \le \pi$. Since $\mathrm{Im}[(dw/d\lambda)\lambda]_{\rho=1} = (\partial\psi_e/\partial\rho)_{\rho=1}$, equation (41) yields

$$g(\varphi) = Q_\infty \sin\varphi - \sum_{j=1}^{\infty} j\, a_j \sin(j\,\varphi) = \left(\frac{\partial \psi_i}{\partial \rho}\right)_{\rho=1}. \tag{42}$$

Truncating the series in (42) at some number N, we can determine all the unknown coefficients $a_j,\ j = 1,\ldots,N$ by using a suitable number of collocation points in $[0,\pi]$.

The interior and exterior flow computations are iterated until ψ_i and ψ_e converge to the same values on the interface γ_{AB}. A linear relaxation approach $\psi_e^{n+1} = (1-f_r)\tilde{\psi}_e^{n+1} + f_r\psi_e^n$ has was adopted for the solution values on the interface γ_{AB} [cf. (37c)] with the under–relaxation factor $f_r \in [0,1]$ chosen heuristically. Continuous families of solutions of (1)–(2) are tracked by modifying the value of the parameter, i.e., α, or ω_0, an then solving the problem again using the solution obtained for the previous parameter value of the initial guess.

5.3 Benchmark Tests

The accuracy of the method was analyzed by comparing the results of the numerical computations to the analytical solution available when $\alpha \to -\infty$, that is when the vortex patch $A(\alpha)$ shrinks to a point vortex (see, for instance, [14]). In this case, the interior solution ψ_i is obtained by modifying equations (36), (37b) and (37c) as follows

$$\begin{aligned}
&\psi_i = \psi^0 + \Gamma\psi^1 && \text{in } \Omega_i,\\
&\psi^0 = -\psi_v && \text{on } \gamma_{AC}\cup\gamma_{CD}\cup\gamma_{DB},\\
&\psi^0 = \psi_e - \psi_v && \text{on } \gamma_{AB},
\end{aligned}$$

where Γ is the vortex circulation and $\psi_v = -\frac{\Gamma}{2\pi}\log|z-z_v|$ is the streamfunction induced by a point vortex located at z_v in an unbounded domain.

The streamline pattern obtained in such a point vortex solution is shown in Figure 5a. The L_2 errors of the numerical solution with respect to the analytical solution computed based on the flow velocity along the separatrix streamline γ_{AB} and the

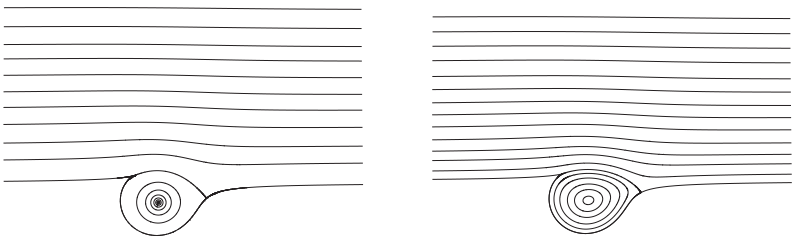

Fig. 5. Streamline patterns for (a) the point vortex equilibrium solution and (b) the corresponding Prandtl–Batchelor solution.

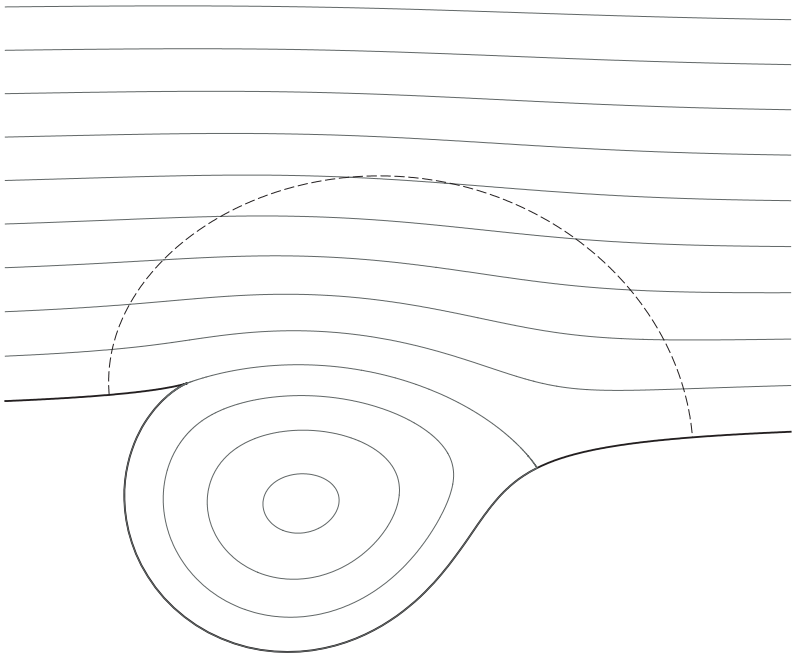

Fig. 6. The interior domain Ω_i in the Batchelor flow.

vortex circulation are in both cases $O(10^{-6})$. Figure 5b represents the corresponding Prandtl–Batchelor flow with a constant nonzero vorticity in the entire recirculation zone computed with the present method. A close–up of the interior region in the Prandtl–Batchelor flow is shown in Figure 6.

We close this Subsection by commenting on the computational efficiency of the proposed method. The main computational cost is due to solution of the interior Poisson problem (38) at each iteration. A fast Poisson solver was adopted from the Fishpack90 library [37]. The computations were done on a PC with the AMD Athlon 64 3000+ 1.81 GHz CPU and with 1 Gb RAM. Examples of the CPU times required to solve the full problem are shown in Table 1 for a 1500×1500 grid and for different values of the relaxation factor f_r. Figure 7 shows the rates of convergence obtained in the solution of this problem with different values of f_r.

f_r	iterations	CPU time $[s]$
0.25	37	630
0.40	10	300
0.50	7	250
0.60	10	570
0.75	19	1270

Table 1
CPU times required to obtain the solution of system (1)–(2) with $\alpha = -0.05$ on a 1500×1500 grid with different values of the under–relaxation factor f_r.

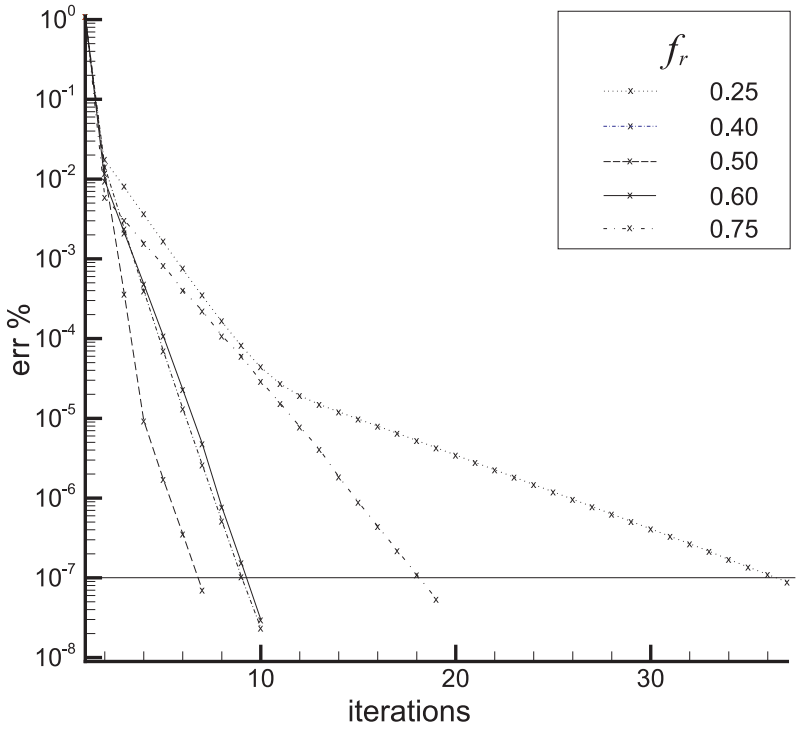

Fig. 7. Rates of convergence of the Steklov-Poincaré algorithm described in Sections 5.1 and 5.2 and obtained in the solution of system (1)–(2) with $\alpha = -0.05$ on a 1500×1500 grid with different values of the under–relaxation factor f_r indicated in the legend. The horizontal line without symbols represents the tolerance used in the termination condition.

6 Numerical Computations of Continuous Families of Solutions

In this Section we present results of numerical computations to illustrate Theorems 3 and 4. We will first analyze the case where the Kutta condition is not imposed and solutions of (1)–(2) can be continued simultaneously with respect to α and ω. Then we will consider the case with Kutta condition (5) imposed, so that solutions of (1)–(2) can be continued with respect to one parameter only. As was argued in Introduction, existence of point–vortex equilibria and of the associated families of

Solution	α	ω	$\lvert A\rvert$	Γ
R	-0.5	-25.481	0.189	-4.811
A_1	-0.646	-25.482	0.221	-5.628
A_2	-0.392	-25.481	0.163	-4.156
B_1	-0.5	-22.456	0.227	-5.103
B_2	-0.5	-28.593	0.156	-4.563

Table 2
Parameters of the reference solution (R) and the perturbed solutions (A_1, A_2, B_1, B_2) for the case when the Kutta condition is not enforced.

steady vortex patches satisfying also the Kutta condition is a nontrivial problem. It becomes particularly involved when the domain boundary possesses a fore–and–aft symmetry. In this regard, it was shown in [14] that in such cases the existence of equilibrium point–vortex configurations depends on the specific form of the conformal map that transforms the domain boundary into the real axis in the transformed domain. Thus, we choose this conformal map in the form

$$z = \frac{\lambda}{a} + b - \frac{1}{5\left(\frac{\lambda}{a} + b + i\right)^5}, \tag{43}$$

where, as explained in Section 5.1, the parameters a and b are determined by requiring that $z_A = z(-1)$, $z_B = z(1)$. In accordance with the criteria derived in [14], formula (43) ensures the existence of equilibrium vortex configurations. In view of the controversy surrounding the question of existence of vortex equilibria in domains with symmetries (cf. Section 1), we find this particular configuration an interesting one. We also add that conformal map (43) is closely related to Ringleb's snow cornice mapping (32), so the Steklov–Poincaré method developed in Section 5 can be used here.

6.1 Continuation in the Absence of the Kutta Condition

As a reference, we consider the solution of problem (1)–(2) corresponding to $\alpha_0 = -0.5$ which, without loss of generality, also satisfies Kutta condition (5). The streamline pattern of this solution is illustrated in Figure 8a. Since the vortex patch boundary is regular, Assumptions (22) are clearly satisfied and, by Theorem 3, this solution can be continued with respect to the parameters. We thus consider two different continuations of the reference solution, namely:

- holding the vorticity ω fixed, and perturbing the boundary value of the streamfunction as $\alpha = \alpha_0 \pm \delta\alpha$, where $\delta\alpha > 0$ is a perturbation (different in each of the two cases); the corresponding solutions A_1 and A_2 are shown in Figures 8c,d, and their locus is represented by the horizontal line in Figure 8b,

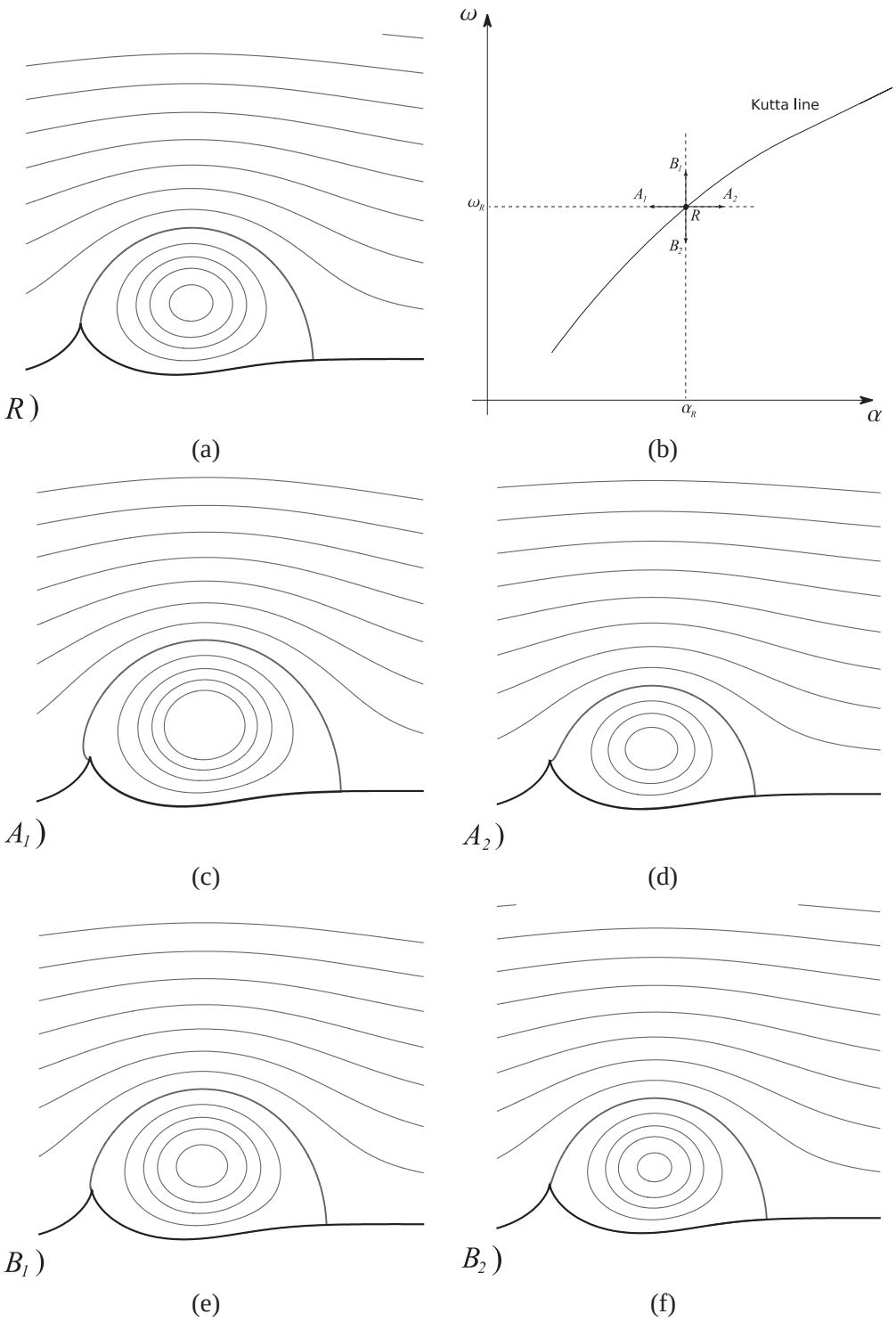

Fig. 8. Streamline patterns in the solutions of system (1)–(2): (a) the reference solution obtained with $\alpha = -0.5$, (c), (d) solutions with unchanged ω and perturbed α, (e), (f) solutions with unchanged α and perturbed ω; thicker lines mark the streamlines bounding the recirculation regions; figure (b) represents schematically the reference solution and the loci of the perturbed solutions in the α–ω plane.

- holding the boundary value α of the streamfunction fixed, and perturbing the vorticity as $\omega = \omega_0 \pm \delta\omega$, where $\delta\omega > 0$ is a perturbation (different in each of the two cases); the corresponding solutions B_1 and B_2 are shown in Figures 8e,f, and their locus is represented by the vertical line in Figure 8b.

All relevant parameters, i.e., $|A|$ and Γ in addition to α and ω of the reference and perturbed solutions are collected in Table 2. We note that while the reference solution has the separation point at the cusp of the obstacle, this is no longer the case for the perturbed solutions.

6.2 Continuation in the Presence of the Kutta Condition

Subject to Kutta condition (5), solutions of system (1)–(2) represent a one–parameter family. In the limit $\alpha \to -\infty$ they approach a point–vortex solution, whereas for $\alpha = \psi_b = 0$ the recirculation region and the vortex region coincide resulting in the Prandtl–Batchelor solution. Boundaries of the vortex region for solutions belonging to this family and corresponding to the intermediate values of α are shown in Figure 9. Since the vortex patch boundaries in each of those solutions are regular, Assumptions (22) are clearly satisfied and, by Theorem 4, each of these solutions can be continued. In Figure 10 we also show the entire streamline pattern for the terminal Prandtl–Batchelor solution obtained for $\alpha = \psi_b$. The locus representing this solution family in the α–ω plane, i.e., the Kutta line, is shown in Figure 11a, whereas the corresponding locus in the $|A|$–Γ plane is shown in Figure 11b. In both Figures one can clearly see the transition from the point–vortex to the Prandtl–Batchelor solution.

7 Conclusions

In this paper we identified the conditions under which vortex–patch solutions of Euler equations (1)–(2) can be continued with respect to both the vorticity ω and value α of the streamfunction defining the vortex boundary. These conditions, given by (22), are satisfied as long as the vortex patch boundary is smooth. In other words, if there exists a smooth vortex patch in equilibrium with the obstacle and characterized by given values of the vorticity ω and the streamfunction α (or, equivalently, the circulation Γ and the patch area $|A|$), then there also exist nearby perturbed solutions in the α–ω, or $|A|$–Γ, plane. A situation in which conditions (22) are not satisfied may arise when the vortex patch boundary has a singularity in the form of a corner, or a cusp (it is known from [20] that these are the only two singularity types possible). Given the structure of the proofs of Theorems 3 and 4, conditions (22) are *sufficient*, but not *necessary*. Therefore, it might in principle happen that vortex patches with singularities of their boundaries could still be continued. On

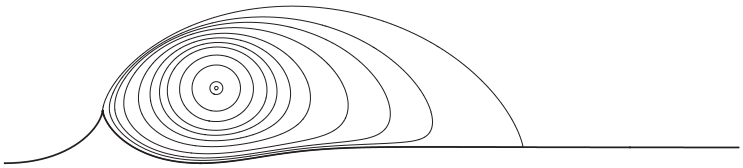

Fig. 9. Family of vortex–patch solutions of system (1)–(2) subject to Kutta condition (5) and connecting the point–vortex solution ($\alpha \to \infty$) with the Prandtl–Batchelor solution ($\alpha = \psi_b = 0$).

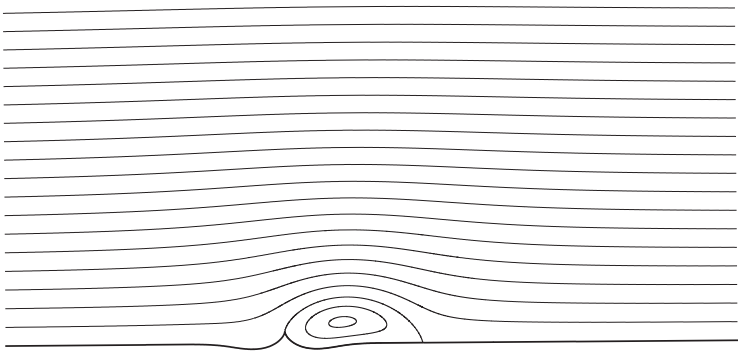

Fig. 10. Streamline pattern of the Prandtl–Batchelor solution ($\alpha = \psi_b$) in which the vortex patch coincides with the recirculation region.

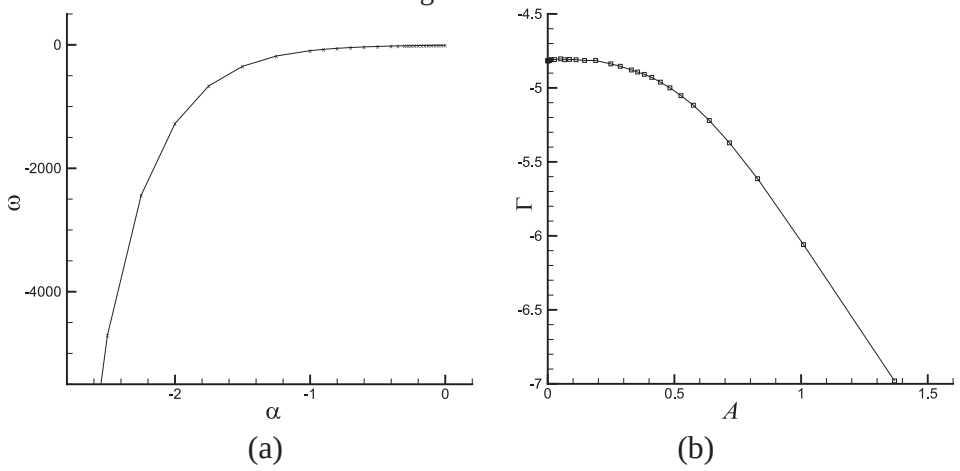

Fig. 11. Loci of solutions of system (1)–(2) satisfying also Kutta condition (5) in (a) ω–α parameter space, and (b) Γ–$|A|$ parameter space.

the other hand, however, all computational results we are aware of and which we reviewed in Section 2 indicate that singular patches represent in fact terminal members of solutions families: in addition to our results presented in Section 6.2 (e.g., Figure 9), this was also observed in [27] for the Sadovskii flow and in [23] for a system of two vortex patches touching at three cusp points. We also add that our analysis did not include the case of a patch with a vortex sheet on the boundary which would require a slight generalization of our approach. While computational evidence for the existence of perturbed vortex–patch solutions has been known for a long time, in this investigation we derived, for the first time to the best of our knowledge, mathematically precise conditions allowing one to predict when such

a continuation is possible. Furthermore, we also show that if the original solution satisfies the Kutta condition, then there exists a nearby vortex patch having, for example, a different area, but still satisfying the Kutta condition.

The methodology we developed in this paper does not allow one to construct neighboring solutions, but only establish their existence. Our results are based on linearizations of governing system (1)–(2), hence they are valid only locally in the neighborhood of the reference solution. In principle, one could attempt to construct neighboring solutions by representing them as a Taylor series with respect to a parameter, and then summing up perturbation variables of increasing orders. However, in addition to the need to establish analyticity of solutions of (1)–(2) with respect to the parameter, this would require the summation of an infinite series which is impractical. Therefore, in actual computations it is much more practical to use methods of numerical continuation, and indeed with such techniques we were able to determine a whole family of vortex–patch solutions connecting the point vortex and the Prandtl–Batchelor solution.

We emphasize that equations (17) and (19) satisfied by the perturbations variables ϕ'_α and ϕ'_ω are the main objects of our analysis. Given the free–boundary nature of governing equation (1)–(2), systematic derivation of these perturbation equations required the use of a special technique, namely, the shape–differential calculus. We remark that these perturbation equations are also of independent interest and may be used to study, for instance, the stability of solutions of (1)–(2).

One of the motivations for this work was to understand the extent to which the existence of a vortex patch solution satisfying the Kutta condition implies the existence of the limiting point vortex solution also satisfying the Kutta condition, or, equivalently, the extent to which the non–existence of such a point vortex solution implies that no steady vortex patch can be found to satisfy the Kutta condition for a specific boundary configuration (cf. Conjecture 1). We made a step towards solving this problem by identifying sufficient conditions for the existence of continuous families of solutions characterized by vortex patches. These conditions, given by equations (22), are satisfied as long as the vortex patch boundary remains regular, i.e., free from geometric singularities such as cusps or corners. While extending our findings to include in a rigorous manner the limiting case of a point vortex (corresponding to $\alpha \to -\infty$ and $\omega \to \infty$) remains an outstanding challenge, the results of computations seem to support the "accretion" scenario. Finally, we note that there is also a range of interesting questions concerning the global structure of the solution manifold. Our hope is that methods of nonlinear functional analysis, such as Fredholm's degree theory, might shed some light on these problem.

Acknowledgments

The authors benefited from fruitful discussions with Walter Craig, David Lannes, Haysam Telib and Oleg Volkov. The third author acknowledges the support through an NSERC Discovery Grant (Canada) and the hospitality of Institut de Mathématiques de Bordeaux where a part of this work was accomplished. The first, second and fourth authors acknowledge the support through the EU Sixth Framework — STREP Project VortexCell2050.

References

[1] H. Choi, W.-P. Jeon, J. Kim, "Control of flow over a bluff body", *Ann. Rev. Fluid Mech.* **40**, 113-139, (2008).

[2] B. Protas, "Vortex dynamics models in flow control problems", *Nonlinearity* **21**, 203-250, (2008).

[3] J. Cox , "The Revolutionary Kasper Wing", *Soaring* **37**, 20–23, (1973).

[4] A. J. Majda and A. L. Bertozzi, *Vorticity and Incompressible Flow*, Cambridge University Press, (2002).

[5] V. V. Sychev, A. I. Ruban, V. V. Sychev and G. L. Korolev, *Asymptotic Theory of Separated Flows*, Cambridge University Press, (1998).

[6] G. Batchelor, "Steady laminar flow with closed streamlines at large Reynolds number", *J. Fluid Mech.* **1**, 177-190, (1957).

[7] G. Batchelor, "A proposal concerning laminar wake behind bluff bodies at large Reynolds numbers", *J. Fluid Mech.* **1**, 388-398, (1957).

[8] J.-Z. Wu, H.-Y. Ma and M.-D. Zhou, "Vorticity and Vortex Dynamics", Springer, (2006).

[9] S. I. Chernyshenko, "Asymptotic theory of global separation", *Appl. Mech. Rev.* **51**, 523–536, (1998).

[10] M. A. Goldshtik, *Vortex Flows* (in Russian), Nauka, (1981)

[11] B. Turkington, "On Steady vortex flow in two dimensions. Part I", *Comm. in Partial Differential Equations* **8**, 999–1030, (1983).

[12] B. Turkington, "On Steady vortex flow in two dimensions. Part II", *Comm. in Partial Differential Equations* **8**, 1031–1071, (1983).

[13] A. Elcrat, B. Fornberg, M. Horn & K. Miller, "Some steady vortex flows past a circular cylinder", *J. Fluid Mech.* **409**, 13-27, (2000).

[14] L. Zannetti L, "Vortex equilibrium in flows past bluff bodies", *J. Fluid Mech* **562** 151–171, (2007).

[15] V. V. Meleshko and H. Aref, "A bibliography of vortex dynamics 1858–1956", *Advances in Applied Mechanics* **41**, 197–292, (2007).

[16] C. Turfus, "Prandtl-Batchelor flow past a flat plate at normal incidence in a channel - inviscid analysis", *J. Fluid Mech.* **249**, 59–72, (1993).

[17] C. Turfus, I. P. Castro "A Prandtl-Batchelor model of flow in the wake of a cascade of normal flat plates", *Fluid Dyn. Res.* **26**,(3), 181–202, (2000).

[18] I. P. Castro, "Weakly stratified laminar flow past normal plates", *J. Fluid Mech.* **454**, 21-46, (2002).

[19] H. M. Wu, E. A. Overman II, and N. J. Zabusky, "Steady–State Solutions of the Euler Equations in Two Dimensions: Rotating and Translating V–States and Limiting Cases. I. Numerical Algorithms and Results", *J. Comp. Phys.* **53**, 42–71, (1984).

[20] E. A. Overman II, "Steady–State Solutions of the Euler Equations in Two Dimensions. II. Local Analysis of Limiting V–States", *SIAM J. Appl. Math.* **46**, 765, (1986).

[21] P. G. Saffman and R. Szeto, "Equilibrium shapes of a pair of equal uniform vortices", *Phys. Fluids* **23**, 2339–2342, (1980).

[22] C. Cerretelli and C. H. K. Williamson, "A new family of uniform vortices related to vortex configurations before merging", *J. Fluid Mech.* **493**, 219–229.

[23] D. Crowdy and J. Marshall, "Growing Vortex Patches", *Phys. Fluids* **16** 3122–3130, (2004).

[24] R. T. Pierrehumbert, "A family of steady, translating vortex pairs with distributed vorticity", *J. Fluid Mech.* **99**, 129–144.

[25] P. G. Saffman and S. Tanveer, "The touching pair of equal and opposite uniform vortices", *Phys. Fluids* **25** 1929–1930, (1982).

[26] V. S. Sadovskii, "Vortex regions in a potential stream with a jump of Bernoulli's constant at the boundary", *Appl. Math. Mech.* **35**, 729–735, (1971).

[27] D. W. Moore, P. G. Saffman and S. Tanveer, "The calculation of some Batchelor flows: The Sadovskii vortex and rotational corner flow", *Phys. Fluids* **31** 978–990, (1988).

[28] R. A. Adams and J. F. Fournier, "Sobolev Spaces", Elsevier, (2005).

[29] D. G. Costa, "An Invitation to Variational Methods in Differential Equations", Birkhäuser, (2007).

[30] L. Gasiński and N. S. Papageorgiou, "Nonlinear Analysis", Chapman & Hall, (2006).

[31] J. Sokolowski and J.–P. Zolésio, *Introduction to Shape Optimization. Shape Sensitivity Analysis*, Springer, (1992).

[32] L. C. Evans, "Partial Differential Equations", AMS, (2002).

[33] F. John, “Partial Differential Equations”, (third edition), Springer, (1978).

[34] A. Quarteroni and A. Valli, *Domain Decomposition Methods for Partial Differential Equations*, Oxford University Press, (1999).

[35] G. F. Carrier, M. Krook and C. E. Pearson, *Functions of a Complex Variables: Theory and Techniques*, SIAM, (2005).

[36] F. O. Ringleb, *Separation control by trapped vortices*, in Boundary Layer and Flow Control (G. V. Lachmann ed.), Pergamon Press (1961).

[37] J. Adams, P. Swarztrauber and R. Sweet, “FISHPACK90 — Efficient FORTRAN Subprograms for the Solution of Separable Elliptic Partial Differential Equations”, `http://www.cisl.ucar.edu/css/ software/fishpack90/`.